ОБЪЕДИНЕННЫЙ
ИНСТИТУТ
ЯДЕРНЫХ
ИССЛЕДОВАНИЙ

Дубна

E2-95-412

A.B.Arbuzov, E.A.Kuraev, N.P.Merenkov[1], L.Trentadue[2]

HARD PAIR PRODUCTION IN LARGE-ANGLE BHABHA SCATTERING

Submitted to «Письма в ЖЭТФ»

[1]Physical-Technical Institute, Kharkov, 310108, Ukraine
[2]Dipartimento di Fisica, Universita di Roma «Tor Vergata» and INFN Sezione di Roma II, via della Ricerca Scientifica, 1, 00133 Roma, Italy

1995

1 Introduction

Large–angle Bhabha scattering (LABS) process ($e^+e^- \to e^+e^-$) is planned to be used for mobile luminosity measurement at electron positron colliders of intermediate energies ($\sqrt{s} \sim 1 \div 3$ GeV). The experimental accuracy of the measurement is planned [1, 2] to have an accuracy better then 0.1%. The absence of the adequate calculations of the cross–section in the frames of the Standard electroweak theory is the motivation of a series of papers devoted to the systematic analytical calculations of the radiative corrections (RC) to the process at the $O(\alpha^2)$ level. Due to the complexity of the problem we separate it into several parts. In this paper we consider the process of the $2 \to 4$ type:

$$e^-(p_1) + e^+(p_2) \to e^-(q_1) + e^+(q_2) + e^-(p_-) + e^+(p_+). \qquad (1)$$

We assume for definiteness that two final particles $e^-(q_1)$ and $e^+(q_2)$ hit the detectors, allowing the angular aperture and the energy thresholds:

$$\Psi_0 < \theta_1, \theta_2 < \pi - \Psi_0, \quad \theta_{1,2} = \widehat{q_{1,2}p_1}, \quad y_{\text{th}} < y_{1,2} < 1, \quad y_{1,2} = \frac{q^0_{1,2}}{\varepsilon}, \qquad (2)$$

where the dead angle Ψ_0 depends on the detector ($\Psi_0 \sim 20^\circ$ for DAFNE [1] and $\Psi_0 \sim 35^\circ$ for CMD–1 [2]), $y_{\text{th}} \gtrsim 0.1$, ε is the beam energy (center–of–mass (CM) reference frame of the initial particles is implied).

In our recent paper [3] the similar problems were considered for the case of small–angle Bhabha scattering (SABS). Our calculations for the LABS case are more complicated compared to the ones for the SABS case at least in three points: *i)* the generalized eikonal form of the amplitude used in the SABS case allows to omit in the consideration all the scattering type Feynman diagrams with more then one photon exchanged in the t–channel; *ii)* the second simplification was connected with the possibility to omit at the $O(\alpha^2)$ level the Feynman diagrams of the annihilation type as well as all contributions connected with Z, W and H bosons; *iii)* and, finally, in the SABS case there was a possibility to omit all terms due to the interference of the "emission from the positron" with "the emission from the electron" (that was valid as for soft as well as for hard particles — photons or pairs). For the LABS case only the possibility to omit heavy boson (Z, W, H) contributions in the $O(\alpha^2)$ order remains.

2 Definitions of Kinematical Regions

There are 36 tree–like Feynman diagrams which describe e^+e^- pair production in the LABS process. A lot of attention was paid to this process in the literature some years ago [4, 5], when different cross–sections were obtained in terms of chiral amplitudes. It was find out that in the case of the general kinematics the cross section has a rather complicated form. Fortunately in the general case, when the angles between each two final particles are not small, the correspondent RC contribution to the Born cross-section will have the magnitude $(\alpha/\pi)^2 \sim 10^{-5}$):

$$\mathrm{d}\sigma^{e\bar{e}\to 2e2\bar{e}} \sim \mathrm{d}\sigma_0^{e\bar{e}\to e\bar{e}}\left(1+O\left(\frac{\alpha^2}{\pi^2}\right)\right) \tag{3}$$

and could be safely omitted working within the accuracy 0.1%. Reinforcements of RC contributions due to pair production appear in the cases when one or two final particles move within a small angle $\theta_i \sim m_e/\varepsilon$ along the direction of one of the tagged (initial or final registered) particles. In these cases one will have logarithmically reinforced contributions of the orders $(\alpha L/\pi)^2$ and $(\alpha/\pi)^2 L$, where $L = \ln s/m_e^2$ is the "large logarithm", $s = 4\varepsilon^2$ ($L \sim 15$ for $\sqrt{s} \sim 1$ GeV). The aim of this paper is to extract the contribution of such a kind, because of their importance at the 0.1% accuracy level.

As the collinear kinematics we call the one when two of final particles (which are not registered) move within the small cone around of the direction of one of the initial particles or around of the direction of the one of the registered final particles:

$$\theta_i < \theta_0, \qquad \frac{m_e^2}{\varepsilon^2} \ll \theta_0 \ll 1, \tag{4}$$

where θ_i, $i = 1, 2$ are the polar angles of the two particles in respect to the chosen direction. As the semi-collinear case we define the kinematics when only one of the non-registered final particles move within such a cone and the second one does not (in respect to all tagged directions). The contribution of the collinear kinematics has the form:

$$a\left(\frac{\alpha}{\pi}(L+\ln\theta_0^2)\right)^2 + b\left(\frac{\alpha}{\pi}\right)^2(L+\ln\theta_0^2), \tag{5}$$

while the semi-collinear one reads

$$\left(\frac{\alpha}{\pi}\right)^2 f(\theta_0)L, \qquad f(\theta_0) = -2a\ln\theta_0^2 + c, \tag{6}$$

where c is finite for $\theta_0 \to 0$. The sum of the two contributions does not depend on the auxiliary parameter θ_0 within the logarithmic accuracy (we omit the terms $(\alpha/\pi)^2 \ln^2\theta_0^2$ and $(\alpha/\pi)^2 \ln\theta_0^2$). The cancelation of the dependence provides one of the tests in our calculations.

Consider now the structure of the collinear region contribution to the cross-section. It could be presented as a sum of the cross sections of hard subprocesses multiplied by so called collinear factors. In the case of the emission of one or two hard collinear photons the hard subprocess is just the Bhabha scattering. That is the manifestation of the known factorization theorem in the simplest form [6].

In the case of pair production besides Bhabha scattering there appear three other type of hard subprocesses: Compton scattering, two-quantum annihilation of the initial particles, and the subprocess of the creation of the final registered particles by two photons, moving close to the directions of the initial beams. Note that this rather complicated form of the factorization theorem appears at first in process under consideration.

The contributions of the semi-collinear regions as well could be expressed in terms of hard subprocesses of the $2 \to 3$ type [6]: a single photon emission in e^+e^- scattering, and the process of pair creation in a photon-electron (-positron) scattering. In Fig. 1 and Fig. 2 we show the kinematical schemes for the collinear and semi-collinear regions (empty circles denote the production of a collinear undetected pair, the full ones — hard subprocesses).

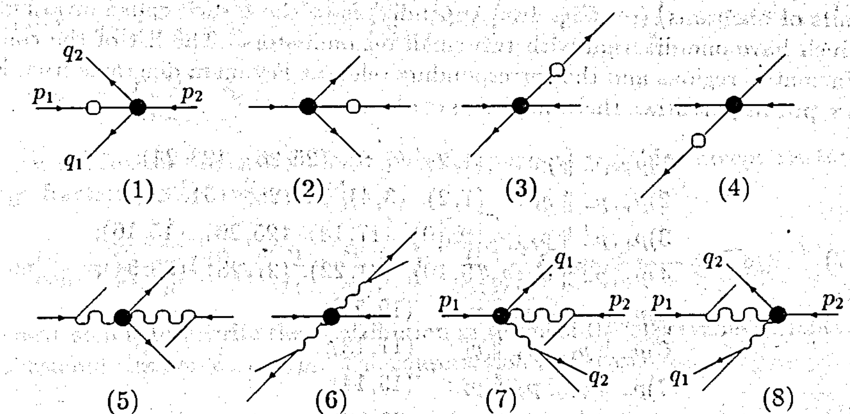

Figure 1: Kinematical diagrams for collinear pair production.

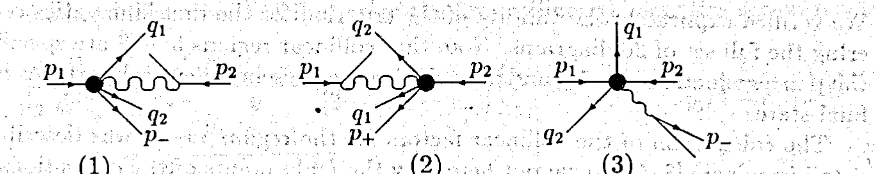

Figure 2: Kinematical diagrams for semi-collinear pair production.

Our method, we believe, save a lot of computation work. Really, instead of 8-fold integration of very complicated expressions with sharp singularities it provides 2(3)-fold integrals of smooth functions in the frames of the same accuracy.

3 Collinear Regions

Consider first the set of collinear kinematics. We will see that there are 8 different cases. As we underlined above the experimental criterion of an event consists in the kinematics of the final particles with at least one electron and one positron moving in large to the beam direction angles in the opposite hemispheres. In the case of the emission of a particle with momentum k moving along the direction of its parent particle with momentum p in the denominator of the matrix element small quantity $2pk$ appears. It is evident that at least two such small denominators are necessary to obtain non-zero contribution integrating over the small phase volume of the two emitted particles in the collinear kinematics ($\mathrm{d}\Gamma_2 \sim \theta_0^4$). Our criterion of the Feynman diagrams selection from the total 36 ones (or from 18 gauge invariant pairs of diagrams) (see Fig. 4 in Appendix) is to chose such gauge invariant sets which have one diagram with two small denominators. The list of the collinear kinematics regions and the corresponding relevant Feynman diagrams from Fig. 4 (we put in parenthes their numbers) reads:

$$
\begin{array}{ll}
1) p_+, p_- \parallel p_1: & (1,2),\ (7,8),\ (25,26),\ (23,24); \\
2) p_+, p_- \parallel q_1: & (1,2),\ (3,4),\ (27,28),\ (31,32); \\
3) p_+, p_- \parallel p_2: & (9,10),\ (17,18),\ (25,26),\ (15,16); \\
4) p_+, p_- \parallel q_2: & (9,10),\ (21,22),\ (27,28),\ (33,34); \\
5) p_- \parallel p_1,\ \ p_+ \parallel p_2: & (19,20); \\
6) p_- \parallel p_1,\ \ p_+ \parallel q_1: & (11,12); \\
7) p_- \parallel q_2,\ \ p_+ \parallel p_2: & (13,14); \\
8) p_- \parallel q_2,\ \ p_+ \parallel q_1: & (29,30).
\end{array}
\quad (7)
$$

We verified explicetely the validity of the criterion for the first kinematics considering the full set of 36 diagrams. Note that collinear regions 5 — 8 are specific for the pair production process and arise due to the presence identical particles in the final state.

The calculation of the collinear factors for the region 1 — 4 was described in detail in papers [8, 9], so we put here only the main points of the derivations. We start from the general form of the cross section in region 1:

$$
\mathrm{d}\sigma^{(1)}_{\mathrm{coll}} = \frac{\alpha^4}{8\pi^4 s} \sum_{\mathrm{spin}} |M^{(1)}|^2 \frac{\mathrm{d}^3 q_1 \mathrm{d}^3 q_2}{4 q_1^0 q_2^0} \frac{\mathrm{d}^3 p_- \mathrm{d}^3 p_+}{4 p_-^0 p_+^0} \delta^4(y p_1 + p_2 - q_1 - q_2), \quad (8)
$$

$$
y = 1 - x_- - x_+, \qquad x_\pm = \frac{p_\pm^0}{\varepsilon},
$$

where

$$
\sum_{\mathrm{spin}} |M^{(1)}|^2 = \frac{4 I^{(1)}}{y\, m_e^4} 16 \left(\frac{s_1}{t_1} + \frac{t_1}{s_1} + 1 \right)^2, \quad (9)
$$

$$
s_1 = ys = 4y\varepsilon^2, \quad t_1 = yt = -2yy_1\varepsilon^2(1 - c_-), \quad c_- = \cos\widehat{q_1 p_1}, \quad y_{1,2} = \frac{q_{1,2}^0}{\varepsilon},
$$

and quantity $I^{(1)}$ has a rather comlicated function of $z_\pm = \varepsilon^2 \theta_\pm^2 / m_e^2$ and $x_\pm$, it is given explicetly in [8, 10].

Transforming the phase volume of the created pair into the form:

$$
\int \mathrm{d}\Phi = \int \frac{\mathrm{d}^3 p_- \mathrm{d}^3 p_+}{4 p_-^0 p_+^0} = \frac{\pi^2}{4} m_e^4 \int\limits_0^{2\pi} \frac{\mathrm{d}\phi}{2\pi} \int\limits_0^{z_0} \mathrm{d}z_+ \int\limits_0^{z_0} \mathrm{d}z_- \int\limits_0^{1-y} \mathrm{d}x_+ \int\limits_0^{1-y-x_-} x_- x_+ \mathrm{d}x_-, \quad (10)
$$

$$
z_0 = \left(\frac{\varepsilon \theta_0}{m_e} \right)^2 \gg 1,
$$

and performing all integrations over pair components variables except its total energy fraction $(1 - y)$, one obtain:

$$
\mathrm{d}\sigma^{(1)}_{\mathrm{coll}} = \frac{2\alpha^4\, \mathrm{d}y}{\pi^2 s\, y} F^{(1)}(y) \left(\frac{s_1}{t_1} + \frac{t_1}{s_1} + 1 \right)^2 \frac{\mathrm{d}^3 q_1 \mathrm{d}^3 q_2}{4 q_1^0 q_2^0} \delta^4(y p_1 + p_2 - q_1 - q_2). \quad (11)
$$

The next step is to rewrite the contribution in terms of the observable variable of the scattered electron c_- and y_1. The conservation law gives:

$$
1 + y = y_1 + y_2, \qquad -1 + y = y_1 c_- + y_2 c_+, \quad (12)
$$

$$
y_1 \sin\theta_- = y_2 \sin\theta_+, \qquad c_+ = \cos\widehat{q_2 p_1} = \cos\theta_+.
$$

The final result for the contribution of the first collinear kinematics region reads:

$$
\frac{\mathrm{d}\sigma^{(1)}}{\mathrm{d}y_1 \mathrm{d}c_-} = \frac{\alpha^4}{s\pi} \frac{F^{(1)}(y, z_0)}{y} \frac{y_1}{[2 - y_1(1 - c_-)]} \left(1 - y_1 \frac{1 - c_-}{2} - \frac{2}{y_1(1 - c_-)} \right)^2, \quad (13)
$$

$$
y = \frac{y_1(1 + c_-)}{2 - y_1(1 - c_-)},
$$

quantity $F^{(1)}(y, z_0)$ could be found in papers [8, 10], it has the following form:

$$
F^{(1)}(y, z_0) = L\left(\frac{1}{2} R(y) L + f(y) \right), \qquad L = \ln z_0, \quad (14)
$$

$$
R(y) = \frac{2}{3} \frac{1 + y^2}{1 - y} + \frac{1 - y}{3y}(4 + 7y + 4y^2) + 2(1 + y)\ln y,
$$

$$
f(y) = \frac{1}{9}\left(-107 + 136y - 6y^2 - \frac{12}{y} - \frac{20}{1 - y}\right) + \frac{2}{3}(-4y^2 - 5y + 1
$$

$$+\frac{4}{y(1-y)})\ln(1-y)+\frac{1}{3}(8y^2+5y-7-\frac{13}{1-y})\ln y-\frac{2}{1-y}\ln^2 y$$
$$+\ 4(1+y)\ln y\ln(1-y)+\frac{2(1-3y^2)}{1-y}\mathrm{Li}_2(1-y),$$
$$\mathrm{Li}_2(x) = -\int\limits_0^x \frac{\mathrm{d}t\ln(1-t)}{t}.$$

We remember the way in which this differential cross-section enters the experimentally observable one:

$$\Delta\sigma^{(1)}_{\mathrm{exp}} = \int\limits_{-c_0}^{c_0}\mathrm{d}c_-\int\limits_{y_{\mathrm{th}}}^{1}\mathrm{d}y_1\Theta(c_0^2-c_+^2)\Theta(y_2-y_{th})\Theta(1-y_2)\frac{\mathrm{d}\sigma^{(1)}_{\mathrm{coll}}}{\mathrm{d}y_1\mathrm{d}c_-}, \qquad (15)$$

where

$$y_2=\frac{1+(1-y_1)^2+y_1(2-y_1)c_-}{2-y_1(1-c_-)}, \quad c_+=\frac{-1+y-y_1c_-}{y_2}, \quad c_0=\cos\Psi_0. \qquad (16)$$

Let us consider as a check that our formula for $\mathrm{d}\sigma_c^{(1)}$ agrees with the corresponding contribution to the SABS cross-section. Really, the correspondence would took place if we took the small angle limit:

$$c_-=1-\frac{\theta_-^2}{2}, \quad \theta_+=y\theta_-, \quad z=\frac{\theta_+^2}{\theta_1^2}, \quad Q_1^2=\varepsilon^2\theta_1^2. \qquad (17)$$

In this way we obtain:

$$\mathrm{d}\sigma^{(1)}=\frac{\alpha^2}{4\pi^2}\frac{4\pi\alpha^2}{Q_1^2}F^{(1)}(y,z_0)\mathrm{d}y\frac{\mathrm{d}z}{z^2}, \qquad (18)$$

this formula agrees with eq. (39) from [3], where two directions were taken into account (we have to note that the expression for $f(y)$ in [3] contains some misprints, they are corrected above).

Exactly the same contribution gives to the cross-section the collinear region 3:

$$\Delta\sigma^{(3)}_{\mathrm{exp}}=\Delta\sigma^{(1)}_{\mathrm{exp}}. \qquad (19)$$

As well the contributions of the collinear regions 2 and 4 are equal:

$$\Delta\sigma^{(2)}_{\mathrm{exp}}=\Delta\sigma^{(4)}_{\mathrm{exp}}, \qquad (20)$$
$$\Delta\sigma^{(2)}_{\mathrm{exp}}=\int\limits_{-c_0}^{c_0}\mathrm{d}c_-\int\limits_{y_{\mathrm{th}}}^{1}\mathrm{d}y_1\frac{\mathrm{d}\sigma^{(2)}_{\mathrm{coll}}}{\mathrm{d}y_1\mathrm{d}c_-}, \qquad y_2=1, \quad c_+=-c_-, \quad y_1=y,$$

$$\frac{\mathrm{d}\sigma^{(2)}}{\mathrm{d}y_1\mathrm{d}c_-}=\frac{\alpha^4}{2s\pi}F^{(2)}(y,z_0)\Big(1-\frac{1-c_-}{2}-\frac{2}{1-c_-}\Big)^2,$$
$$F^{(2)}(y,z_0)=-yF^{(1)}(\frac{1}{y},z_0y^2)=L\Big(\frac{1}{2}R(y)L+2R(y)\ln y+f_1(y)\Big),$$
$$f_1(y)=\frac{1}{9}(-116+127y+12y^2+\frac{6}{y}-\frac{20}{1-y})+\frac{2}{3}(-4y^2-5y+1$$
$$+\frac{4}{y(1-y)})\ln(1-y)+\frac{1}{3}(8y^2-10y-10+\frac{5}{1-y})\ln y-(1+y)\ln^2 y$$
$$+\ 4(1+y)\ln y\ln(1-y)+\frac{2(3-y^2)}{1-y}\mathrm{Li}_2(1-y).$$

Again one can check the correspondence of this result with the case of SABS (see eq. (39) in [3]).

We underline that neglecting terms of the order α^2/π^2 permits us within the accuracy of 0.1% to express the contribution to σ_{exp} in terms of two-fold integrals from smooth fuctions.

(1) (2)

Figure 3: Diagrams for collinear factors in a space-like kinematics (1) and in a time-like one (2).

Consider now the collinear region 5 (see Fig. 1(5)) in which two of the final particles moves close to the directions of the initial beams and the registered pair is created by two almost real photons moving also very close to the initial particles directions. The way of the collinear factors calculations in this case could be considered as an essential generalization of the Weizsakker–Williams approximation [12, 13]. Let us consider the block of the kinematical diagram Fig. 1(5) which describes the emission of an undetected fermion and an almost real photon (both close to the initial direction), the photon then enters a hard block (see Fig. 3(1)). The corresponding matrix element reads:

$$M=\frac{1}{q^2}J_\nu g^{\mu\nu}I_\mu, \qquad J_\nu=\bar{u}(p_1')\gamma_\nu u(p_1), \qquad (21)$$

where I_μ is the current corresponding to the hard block. Let us expand, following V. Sudakov [11], the 4-momentum of the emitted fermion:

$$p_1' = \alpha\tilde{p}_2+\beta\tilde{p}_1+p'_{1\perp}, \qquad p'_{1\perp}p_1=p'_{1\perp}p_2=0, \qquad (22)$$
$$\tilde{p}_{1,2} = p_{1,2}-p_{2,1}\frac{m^2}{s}, \qquad s=2p_1p_2\gg m^2.$$

4-momentums $\tilde{p}_{1,2}$ are almos light–like. Parameter β here is a quantity of the order of unity, it has the sense of the energy fraction of the scattered electron; $1-\beta$ is the energy faction of our almost real photon. $p'_{1\perp}$ is the two dimensional vector describing the transverse in respect to the initial direction components of the scattered electron momentum (and further we sign transverse momentum components using symbol $\perp$). Parameter $\alpha = ((p_1)^2+m^2)/(s\beta)$ is small: $\alpha \ll 1$. It could found from the mass shell condition for the scattered electron: ${p'_1}^2 = m^2$. In that way we obtain also the usefull equation:

$$q^2 = -\frac{((p'_{1\perp})^2 + m^2(1-\beta)^2)}{\beta} < 0. \tag{23}$$

Representing identically the metric tensor, entering the photon Green function, in the form:

$$g^{\mu\nu} = g_\perp^{\mu\nu} + \frac{2}{s}(p_1^\mu p_2^\nu + p_1^\nu p_2^\mu), \tag{24}$$

we note that it could be effectively writtebn in the form:

$$g^{\mu\nu} \approx g_\perp^{\mu\nu} + \frac{2}{s} p_1^\mu p_2^\nu, \tag{25}$$

since the contribution of the omitted term is suppresed by an additional factor of the order q^2/s. Taking that into account, one obtains:

$$M = \frac{1}{q^2}\{(JI)_\perp + \frac{2}{s}(Jp_2)(-\frac{Ip'_{1\perp}}{1-\beta})\}, \tag{26}$$

where the current conservation condition

$$Iq = I(\alpha_1 p_2 + (1-\beta)p_1 + q_\perp) \approx I((1-\beta)p_1 + q_\perp) = 0 \tag{27}$$

was used. Perform now the summation over fermion spin states:

$$\sum_{\text{spin}} |(JI)_\perp|^2 = \mathrm{Tr}\,(\hat{p}'_1 + m)\hat{I}_\perp(\hat{p}_1+m)\hat{I}_\perp = -2q^2 I_\perp^2 > 0, \tag{28}$$

$$\sum_{\text{spin}} |Jp_2|^2 = 2s^2\beta, \qquad \sum_{\text{spin}} (Jp_2)(JI)^*_\perp = 2s(q_\perp I_\perp), \qquad q_\perp = -p'_{1\perp}.$$

So, we obtain:

$$\sum_{\text{spin}} |M|^2 = \frac{1}{(q^2)^2}[-2q^2 I_\perp^2 + \frac{8}{(1-\beta)^2}(p'_{1\perp} I_\perp)^2], \tag{29}$$

where q^2 should be taken from eq. (23). The phase volume of the scattered electron could be presented in the form:

$$\int \frac{d^3 p'_1}{2\varepsilon'_1} = \int \frac{d\beta}{2\beta} \int \frac{d\phi}{2\pi} 2\pi \int_0^{(\epsilon\beta\theta_0)^2} \frac{d(p'_{1\perp})^2}{2}. \tag{30}$$

Then we carry out a simple integration and obtain:

$$\int \sum_{\text{spin}} |M|^2 \frac{d^3 p'_1}{2\varepsilon'_1} = \pi (I_\perp)^2 Q(\beta, z_0) d\beta, \tag{31}$$

where the collinear factor $Q(\beta, z_0)$ for a space–like virtual photon has the form:

$$Q(\beta, z_0) = \frac{1+\beta^2}{1-\beta}[L + 2\ln\frac{\beta}{1-\beta}] - \frac{2\beta}{(1-\beta)^2}. \tag{32}$$

Now we are ready to calculate the cross–section in the collinear region 5, where we have two collinear factors $Q(\beta, z_0)$. Besides them we need the summed over spin states matrix element square of the hard block — of the hard e^+e^- pair creation by two photons:

$$\gamma((1-\beta_1)p_1) + \gamma((1-\beta_2)p_2) \to e_+(q_2) + e_-(q_1). \tag{33}$$

Taking the phase volume in terms of the detected electron in the form:

$$d\beta_2 \frac{d^3q_1 d^3q_2}{2q_1^0 2q_2^0}\delta^4(q_1 + q_2 - p_1(1-\beta_1) - p_2(1-\beta_2)) = \frac{\frac{\pi}{2} y_1 dy_1 dc_-}{2\beta_1 - y_1(1+c_-)}, \tag{34}$$

we obtain for the cross–section

$$\begin{aligned} \frac{d\sigma^{(5)}_{\text{coll}}}{dy_1 dc_-} &= \frac{\alpha^4}{2\pi s}\int_0^1 \frac{d\beta_1 2y_2(1-c_-c_+)}{\beta_1^2\beta_2^2(2\beta_1 - y_1(1+c_-))y_1(1-c_-^2)} \\ &\times \{(1+(1-\beta_1)^2)(L + 2\ln\frac{1-\beta_1}{\beta_1}) - 2(1-\beta_1)\} \\ &\times \{(1+(1-\beta_2)^2)(L + 2\ln\frac{1-\beta_2}{\beta_2}) - 2(1-\beta_2)\}, \end{aligned} \tag{35}$$

where

$$2\beta_1 - y_1(1+c_-) > 0, \qquad ,\beta_2 = \frac{y_1\beta_1(1-c_-)}{2\beta_1 - y_1(1+c_-)}, \tag{36}$$

$$y_2 = \frac{2\beta_1^2 + y_1(y_1 - 2\beta_1)(1+c_-)}{2\beta_1 - y_1(1+c_-)}, \qquad c_+ = \frac{1}{y_2}(\beta_1 - \beta_2 - y_1 c_-).$$

For the hard block we used the followin expression:

$$\sum_{\text{spin}} |M^{\gamma\gamma\to e^+e^-}|^2 \sim \frac{t_1}{u_1} + \frac{u_1}{t_1} = \frac{y_1(1-c_-)}{y_2(1-c_+)} + \frac{y_2(1-c_+)}{y_1(1-c_-)} = \frac{2y_2(1-c_+c_-)}{y_1(1-c_-^2)}. \quad (37)$$

And for the contribution to the *experimental* cross–section we obtain

$$\Delta\sigma^{(5)} = \int_{y_{\rm th}}^{1} dy_1 \int_{-c_0}^{c_0} dc_- \frac{d\sigma^{(5)}_{\rm coll}}{dy_1 dc_-} \Theta(y_2 - y_{\rm th})\Theta(1-y_2)\Theta(c_0^2 - c_+^2). \quad (38)$$

The similar situation takes place for the collinear kinematics 6, when the initial electron and positron annihilate into two almost real photons, which then convert into two electron–positron pairs.

The matrix element describing the emission of a time–like almost real photon with subsequent its convertion into a pair (see Fig. 3(2)) has the form:

$$M = \frac{g^{\mu\nu}}{k^2} I_\mu J_\nu, \qquad J_\nu = \bar{v}(p_-)\gamma_\nu u(q_+), \quad (39)$$

We use again the Sudakov representation for the momenta of the pair components and of the photon:

$$g^{\mu\nu} \approx g_\perp^{\mu\nu} + \frac{2}{s_1} q^\nu q_+^\mu, \quad q^2 = 0, \quad 2qq_+ = s_1, \quad (40)$$

$$p_- = \alpha_1 q + \beta_1 \tilde{q}_+ + (p_-)_\perp, \qquad \tilde{q}_+ = q_+ - q\frac{m^2}{s_1},$$

$$k = q_+ + p_- = \alpha_2 q + \beta_2 \tilde{q}_+ + k_\perp, \qquad \beta_1 = \beta_2 - 1 > 0.$$

The current conservation condition here reads:

$$kI \approx (\beta_1 \tilde{q}_+ + p_-^\perp) I = 0. \quad (41)$$

Using the above definitions we get the summed over spin states matrix element square in the following form:

$$\sum_{\text{spin}} |M|^2 = 2\frac{(I^\perp)^2}{(k^2)^2} \frac{[(1+(\beta_2-1)^2)(k^\perp)^2 + m^2\beta_2^4]}{\beta_2^2(\beta_2-1)}, \quad k^2 = \frac{(k^\perp)^2 + m^2\beta_2^2}{\beta_2 - 1} > 0. \quad (42)$$

Integrating over the transverse momentum components $(p_-)_\perp$ of the electron from the created pair, we obtain:

$$\int \frac{d^2 p_-^\perp}{2p_-^0} \sum_{\text{spin}} |M|^2 = \frac{\pi (I_\perp)^2 d\beta_2}{\beta_2^2} \{(1+(\beta_2-1)^2)(L + 2\ln(y_2(1-\frac{1}{\beta_2}))) \quad (43)$$
$$+ \ 2(\beta_2 - 1)\}.$$

Note, that due to the character of the hard $e^+e^- \to \gamma\gamma$ block we have $k_1^0 = k_2^0 = \varepsilon$ and the relation between the detected positron energy fraction $y_2 = q_+^0/\varepsilon$ and parameter β_2:

$$\beta_2 = \frac{1}{y_2}. \quad (44)$$

The cross–section for the collinear region 6 takes the form:

$$\frac{d\sigma^{(6)}_{\rm coll}}{dy_1 dc_- dy_2} = \frac{\alpha^4}{4\pi s}\frac{1+c_-^2}{1-c_-}\left\{(y_1^2 + (1-y_1)^2)(L + 2\ln(y_1(1-y_1))) + 2y_1(1-y_1)\right\}$$
$$\times \left\{(y_2^2 + (1-y_2)^2)(L + 2\ln(y_2(1-y_2))) + 2y_2(1-y_2)\right\}. \quad (45)$$

The corresponding contribution to the experimentally observable cross section has the following form:

$$\Delta\sigma^{(6)} = N \int_{y_{\rm th}}^{1} dy_1 \int_{y_{\rm th}}^{1} dy_2 \int_{-c_0}^{c_0} dc_- \frac{d\sigma^{(6)}_{\rm coll}}{dy_1 dc_- dy_2}, \qquad c_+ = -c_-. \quad (46)$$

Quantity N depends on the concrete experimental set–up. Namely, $N = 1/2$ when one requires to register two leptons with opposite charges going back–to–back. In a charge–blind set–up one would have $N = 1$.

Consider now two remaining collinear region (7,8). They contain as a hard block the Compton scattering amplitude. Combining the expressions for the collinear factors for time–like and space–like photons one obtains:

$$\Delta\sigma^{(7)} = \Delta\sigma^{(8)} = \int_{y_{\rm th}}^{1} dy_1 \int_{-c_0}^{c_0} dc_- \frac{\sigma^{(8)}}{dy_1 dc_-} \Theta(1-y_2)\Theta(y_2 - y_{\rm th})\Theta(c_0^2 - c_+^2), \quad (47)$$

$$\frac{\sigma^{(8)}}{dy_1 dc_-} = \frac{\alpha^4}{2\pi s} \int_{\beta_{\rm 1min}}^{1} \frac{d\beta_1}{\beta_1^2\beta_2^2(1+\beta_1 + c_-(1-\beta_1))}\left(\frac{y_2(1-c_+)}{2} + \frac{2}{y_2(1-c_+)}\right)$$
$$\times \left\{(1+(1-\beta_1)^2)(L + 2\ln\frac{1-\beta_1}{\beta_1}) - 2(1-\beta_1)\right\}$$
$$\times \left\{(1+(\beta_2-1)^2)(L + 2\ln(y_2\frac{(\beta_2-1)}{\beta_2})) + 2(\beta_2-1)\right\},$$

$$\beta_2 = \frac{2\beta_1}{y_1(1+\beta_1+(1-\beta_1)c_-)}, \qquad y_2 = \frac{1+\beta_1^2 + c_-(1-\beta_1^2)}{1+\beta_1 + c_-(1-\beta_1)},$$

$$c_+ = \frac{1}{y_2}[\beta_1 - 1 - \beta_2 y_1 c_-], \qquad \beta_{\rm 1min} = \frac{y_1(1+c_-)}{2 - y_1(1-c_-)}.$$

4 Semi–Collinear Regions

The differential cross–section of the pair production process in large–angle Bhabha scattering (see Fig. 2) has the following form:

$$\begin{aligned}\Delta\sigma_{\text{s-coll}} &= 2\frac{\alpha}{2\pi}L\int\limits_{0}^{1-\beta_0}\frac{d\beta(1+\beta^2)}{1-\beta}\Sigma_1(\Omega_1,\Omega_2,\Omega_+,\theta_0) \\ &\times\ d\sigma(\gamma(p_1(1-\beta))+e^+(p_2)\to e^+(p_+)+e^+(q_2)+e^-(q_1)) \\ &+\ \frac{\alpha}{2\pi}L\int\limits_{1}^{1/y}\frac{d\beta}{\beta^2}(1+(\beta-1)^2)\Sigma_2(\Omega_1,\Omega_2,\theta_0) \\ &\times\ d\sigma(e^-(p_1)+e^+(p_2)\to e^-(q_1)+e^+(q_2)+\gamma(\beta p_+)),\end{aligned} \tag{48}$$

where we used the collinear factors considered above within the logarithmic accuracy, $y=p_+^0/\varepsilon$, and the hard cross sections [6] are:

$$\begin{aligned}d\sigma^{\gamma(q)+e^+(p_2)\to e^+(p_+)+e^+(q_2)+e^-(q_1)} &= \frac{(4\pi\alpha)^3}{16(2\pi)^5 2qp_2}\frac{1}{p_2p_+\,p_2q_2\,q_1q_2\,p_+q_1} \\ &\times(p_2q_2\,q_1p_+((p_2q_2)^2+(q_1p_+)^2)+p_2p_+\,q_1q_2((q_1q_2)^2+(p_2p_+)^2) \\ &+p_2q_1\,q_2p_+((p_2q_1)^2+(q_2p_+)^2)) \\ &\times\left(\frac{2p_2p_+}{p_2q\,p_+q}+\frac{2p_2q_2}{p_2q\,q_2q}+\frac{2q_1p_+}{q_1q\,p_+q}+\frac{2q_1q_2}{q_1q\,q_2q}-\frac{2p_2q_1}{p_2q\,q_1q}-\frac{2p_+q_2}{p_+q\,q_2q}\right) \\ &\times\delta^4(q+p_2-p_+-q_1-q_2)\frac{d^3q_1d^3q_2d^3p_+}{q_1^0q_2^0p_+^0},\end{aligned} \tag{49}$$

$$\begin{aligned}d\sigma^{e^-(p_1)+e^+(p_2)\to e^-(q_1)+e^+(q_2)+\gamma(q)} &= \frac{(4\pi\alpha)^3}{16(2\pi)^5 2p_1p_2}\frac{1}{p_1p_2\,q_1q_2\,p_1q_1\,p_2q_2} \\ &\times(p_1p_2\,q_1q_2((p_1p_2)^2+(q_1q_2)^2)+p_1q_1\,p_2q_2((p_1q_1)^2+(p_2q_2)^2) \\ &+p_1q_2\,p_2q_1((p_1q_2)^2+(p_2q_1)^2)) \\ &\times\left(\frac{2p_1p_2}{p_1q\,p_2q}+\frac{2q_1q_2}{q_1q\,q_2q}+\frac{2p_1q_1}{p_1q\,q_1q}+\frac{2p_2q_2}{p_2q\,q_2q}-\frac{2p_1q_2}{p_1q\,q_2q}-\frac{2p_2q_1}{p_2q\,q_1q}\right) \\ &\times\delta^4(p_1+p_2-q-q_1-q_2)\frac{d^3q_1d^3q_2d^3q}{q_1^0q_2^0q^0}.\end{aligned} \tag{50}$$

$1-\beta_0$ in eq. (48) is the minimum energy fraction of the virtual photon in the pair creation process $\gamma^*\bar{e}\to e\bar{e}\bar{e}$ provided that fermions with momenta q_1 and q_2 to be detected. Multipliers Σ_1 and Σ_2 provide the emission angles of every final state fermion in respect to the beam directions and to each other fermion to be larger then θ_0. Note that because of the integration over the phase space of the final particles the identity of two positrons is accounted automatically. The numerical integration of $\Delta\sigma_{\text{s-coll}}$ (48) and different contributions to $\Delta\sigma_{\text{coll}}$ (see eqs. (15,20,38,46,47)) will show that the total sum does not depend on the auxiliary parametr θ_0.

5 Conclusions

So, we considered the process of an additional e^+e^- pair production in the large–angle Bhabha scattering. We obtained the differential cross–sections within the logarithmic accuracy. They could be used in a wide range of experimental arrangements. Our approach gives analytical expressions as for the leading contributions as well as for the next–to–leading ones. That provides a control of the theoretical accuracy within 0.1%.

Note that in the leading logarithmic approximation, i.e. for the terms of the order $(\alpha L)^2$, the parton picture of the cross–section is valid: that could be just seen from the above expressions for different collinear kinematics.

Radiative corrections to the considered process, i.e. terms of the order $(\alpha L)^3$ could be obtained using the renormalization group methods. But their contribution is beyond the required accuracy.

The process of the production of two different fermion–antifermion pairs in e^+e^- collisions is of interest for Standard Model testing. As for the problem of the luminosity measurement we suggest that the case of a heavy pair production could be extracted experimentally.

Acknowlegement

We are grateful for usefull discussions and criticism to partipants of Novosibirsk Budker–INP theoretical seminar. The work was supported in part by INTAS grant 93–1867. One of us (A.B.A.) is thankful to the Royal Swedish Academy of Sciences for the financial support via an ICFPM grant.

Appendix

Here we present the full set of 36 Feynman diagrams describing the real e^+e^- pair production in the large–angle Bhabha scattering process.

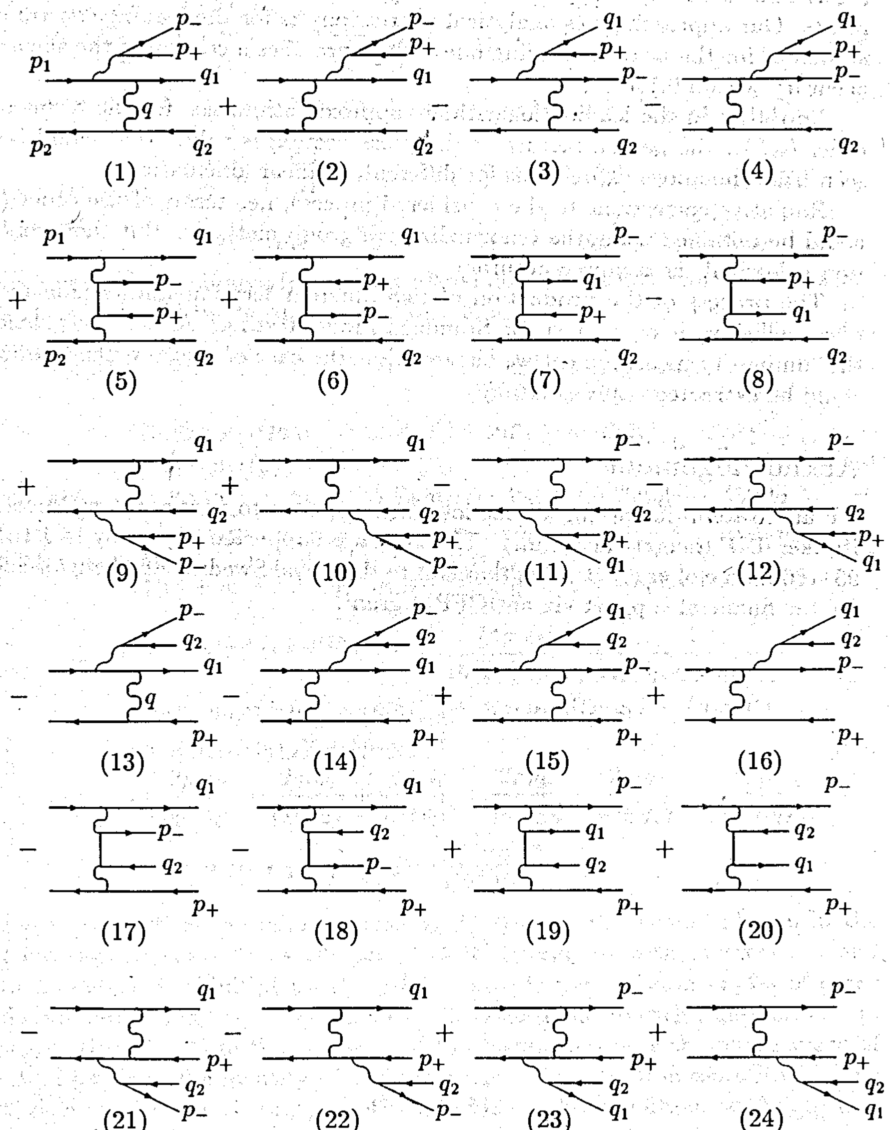

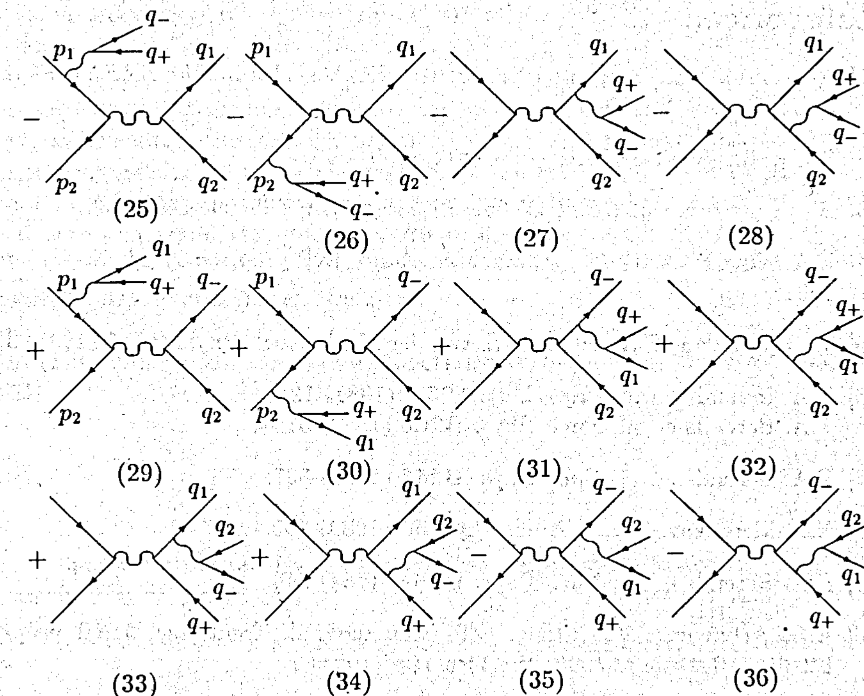

Figure 4: Feynman diagrams for real pair production.

References

[1] A. Aloisio et al., preprint LNF-92/019 (IR); see also in *The DAFNE Physiks Hadbook* Vol. 2, 1993.

[2] S.I. Dolinsky et al., Phys. Rep. **202**, (1991) 99.

[3] A. Arbuzov et. al, *CERN Yellow Report,* CERN 95-03 (1995) 369.

[4] E.A. Kuraev, A.N. Pyoryshkin, V.S. Fadin, INP preprint 89-91, Novosibirsk, 1991.

[5] W. Beenakker, F.A. Berends, S. van der Mark, Nucl. Phys. **B349** (1991) 323.

[6] F.A. Berends et al., Phys. Lett. **103 B**(1981) 124 ;
F.A. Berends et. al, Nucl. Phys. **B206** (1982) 61.

[7] F.A. Berends et. al, Nucl. Phys. **B253** (1983) 537.

[8] N.P. Merenkov, Sov. J. Nucl. Phys. **50** (1989) 469.

[9] F.A. Berends et. al, Nucl. Phys. **B264** (1984) 243.

[10] A.B. Arbuzov, E.A Kuraev, N.P. Merenkov, L. Trentadue, JINR preprint E2-95-110, Dubna, 1995; JhETPh **108** (1995) 1.

[11] V.V. Sudakov, ZhETPh, **30** (1974) 87.

[12] V.N. Baier, V.S. Fadin, V.A. Khoze, Nucl. Phys. **B65** (1973) 381.

[13] A.I. Akhiezer and V.B. Berestezki, *Quantum Electrodynamics,* (in russian) Moscow: Nauka, 1981.

Received by Publishing Department
on September 22, 1995.